

Two-Component Axisymmetric Wave-Energy Absorber – Analysis of Dynamics and Geometric Proportions

Christophe Cochet* and Ronald W. Yeung†

Department of Mechanical Engineering
University of California at Berkeley, Berkeley, CA 94720-1740, USA
E-mail: christophe.cochet@berkeley.edu & rwyeung@berkeley.edu

1 Introduction

The present article focuses on the development of a two-component design for the UC Berkeley wave-energy absorber [1]. The first design, for bench testing and evaluation, was a single floater heaving relative to a fixed platform. A two-component system was designed to allow operation in open ocean without any secondary support system. This is achieved by adding to the original, single vertical cylinder an outer floater of toroidal shape. It is allowed to move along the inner cylinder by a sliding mechanism that constrains the cylinders to a vertical relative motion. The inner cylinder is moored to the seabed. Yeung [2] and Chau and Yeung [3] studied the hydrodynamics of a floating cylinder (single or compound) in heave motion. In parallel efforts to their work, the motion study of the two-component design is pursued and helps to guide the choice of a geometry for the outer cylinder. The goal of this work is to optimize wave-energy extraction. To start with, the 3DoF (surge, heave, and pitch) motion of the two-body system is first examined. Then, the heave motion of the outer cylinder is analysed in order to obtain, in the last stage, a geometry (radii and drafts of cylinders) which optimizes the power extraction. For this purpose, the linear-generator influence is modelled as a dashpot damper and the efficiency evaluated in terms of capture width is used.

2 Dynamics of a moored compound cylinder

We consider a compound-cylinder device constituted of a tethered inner cylinder (of radius a_1 and draft d_1) and an outer cylinder (of radius a_2 and draft d_2) sliding along the inner floater. The global system surges with a displacement $l \sin \beta(t)$ and pitches about \bar{O} with an angle $\alpha(t)$. The outer cylinder slides with displacement $\zeta_3(t)$. Figure 2 defines the geometry of the system. G_1 and G_2 are the centers of gravity of the

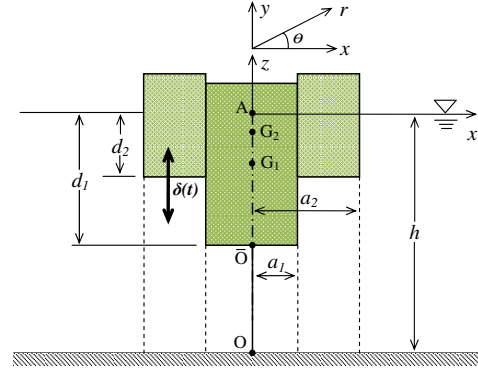


Figure 1: Definition of the compound-cylinder device; $\delta \equiv \zeta_3$ in text.

cylinders, and A the point of intersection of the central axis of the cylinders with the calm water surface. Motion occurs in the Oxz plane. The goal is to determine the motion of the system (described by α , β , and ζ_3) and the contact forces between the two components of the system.

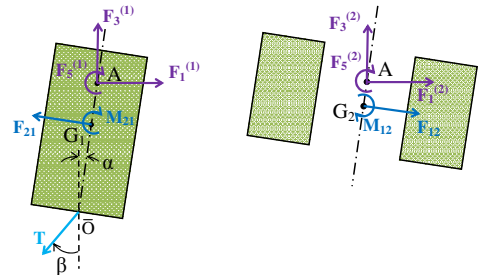


Figure 2: Free-body diagrams of the compound-cylinder components.

The force $F_i^{(j)}$ represents the fluid force (wave-exciting + hydrostatic + added mass + fluid damping) in the i -th direction for the j -th cylinder. The force exerted by the outer cylinder on the inner cylinder is noted F_{21} . Its opposite, F_{12} , is the force of the inner cylinder on the outer cylinder. The moments M_{12} and M_{21} are defined in the same manner. These forces and moments are called connecting forces and moments and are assumed to be of first order when compared to

*Current address: Sophia Conseil, Ingénierie & Innovation, Paris, France

†Correspondence author

hydrostatic forces and moments. The fully nonlinear equations can be developed.

However, once linearized, the equations of motion (two coupled and one independent) can be written in a compact form, with the unknowns of our problem (the displacement variables α , β , ζ_3) regrouped on the left-hand side of the equations¹:

$$(a_{11} + d_{11})\ddot{\beta} + (a_{12} + d_{12})\ddot{\alpha} + (a_{21} + d_{21})\dot{\beta} + (a_{22} + d_{22})\dot{\alpha} + b_0\beta = F_1^{(1)exc} + F_1^{(2)exc} \quad (1)$$

$$(c_{11} + f_{11})\ddot{\beta} + (c_{12} + f_{12})\ddot{\alpha} + (c_{21} + f_{21})\dot{\beta} + (c_{22} + f_{22})\dot{\alpha} + (c_{32} + f_{32})\alpha = F_5^{(1)exc} + F_5^{(2)exc} \quad (2)$$

$$e_{13}\ddot{\zeta}_3 + e_{23}\dot{\zeta}_3 + e_{33}\zeta_3 = F_3^{(2)exc} \quad (3)$$

The expressions for the forces T , F_{12} , and M_{12} can also be obtained:

$$F_{12} = \frac{1}{2} \left[F_1^{(1)exc} - F_1^{(2)exc} + (d_{11} - a_{11})\ddot{\beta} + (d_{12} - a_{12})\ddot{\alpha} + (d_{21} - a_{21})\dot{\beta} + (d_{22} - a_{22})\dot{\alpha} - b_0\beta \right] \quad (4)$$

$$M_{12} = \frac{1}{2} \left[F_5^{(1)exc} - F_5^{(2)exc} + (f_{11} - c_{11})\ddot{\beta} + (f_{12} - c_{12})\ddot{\alpha} + (f_{21} - c_{21})\dot{\beta} + (f_{22} - c_{22})\dot{\alpha} + (f_{32} - c_{32})\alpha \right] \quad (5)$$

$$T = F_3^{(1)exc} + b_0 \quad (6)$$

3 Surge and pitch motion of a compound cylinder

Thanks to the decoupling of the heave motion from the surge and pitch motion, the analysis of this latter can be done by considering the device to be a single-body system: both cylinders share the same amplitude and phase for the surge motion, as well as for the pitch motion, whereas the outer cylinder heaves independently of the other motions. Thus an exciting force and hydrodynamic coefficients common to this single-body system can be defined and are noted with the superscript (C).

It is relatively straight-forward to show that the equations describing the surge and pitch motion of this

¹The coefficients $a_{ij}, b_0, c_{ij}, d_{ij}, e_{ij}$, and f_{ij} , as well as $\tilde{a}_{ij}, \tilde{b}_0, \tilde{c}_{ij}$, can be expressed in terms of hydrodynamic coefficients, mass distribution parameters and geometric dimensions of the system.

single-body system are¹:

$$\tilde{a}_{11}\ddot{\beta} + \tilde{a}_{12}\ddot{\alpha} + \tilde{a}_{21}\dot{\beta} + \tilde{a}_{22}\dot{\alpha} + \tilde{b}_0\beta = F_1^{(C)exc} \quad (7)$$

$$\tilde{c}_{11}\ddot{\beta} + \tilde{c}_{12}\ddot{\alpha} + \tilde{c}_{21}\dot{\beta} + \tilde{c}_{22}\dot{\alpha} + \tilde{c}_{32}\alpha = F_5^{(C)exc} \quad (8)$$

One can observe that, for a fixed geometry and frequency of operation, the surge-and-pitch motion will only depend on the mass distribution of the compound cylinder, i.e. the parameters m_1, m_2, l_1 and l_2 . In addition, these parameters are constrained by physical considerations: m_1 cannot exceed $\rho\forall_1$ (buoyancy of inner cylinder); the difference $(\rho\forall_1 - m_1)g$ characterizes the tension in the mooring cable; m_2 is fixed by the geometry of the outer cylinder ($m_2 = \rho\forall_2$). Thus, the design procedure should include a careful ballasting of the system.

4 Heave motion of a compound cylinder

In this section, we assume a compound-cylinder device whose inner cylinder is moored and outer cylinder is restricted to heave motion. In this situation, the inner cylinder is effectively fixed. All the variables relate to the outer floater, except when specified.

Given that the motion is time-harmonic, Eqn. (3) yields the Response Amplitude Operator (RAO)²:

$$\overline{\mathcal{A}}_3 = \frac{\mathcal{A}_3}{A} = \frac{\overline{X}_3}{(\gamma - \sigma^2(\overline{m} + \overline{\mu}_{33})) - i\sigma^2\overline{\lambda}_{33}}, \quad (9)$$

as well as the non-dimensional resonance frequency, given by the implicit solution:

$$\overline{\sigma}_{res} = \sqrt{\gamma/(\overline{m} + \overline{\mu}_{33}(\overline{\sigma}_{res}))}. \quad (10)$$

In order to take into account viscosity, one can introduce a factor f_{vis} in the expression of the viscous damping:

$$\lambda_T = (1 + f_{vis})\lambda_{33}. \quad (11)$$

This new factor f_{vis} can be determined either by numerical simulation [4], or through free-motion and free-decay tests of a model tests [1].

Finally, when the generator is connected to the device, an additional damping force (with coefficient B_g) has to be considered, with λ_T to be replaced by λ_{Tg} :

$$\lambda_{Tg} = (1 + \tilde{f})\lambda_T \quad \text{with} \quad \tilde{f} = \frac{B_g}{\lambda_T}. \quad (12)$$

²Non-dimensional parameters: $\overline{X}_3 = X_3/(\pi\rho g a_2^2)$, $\gamma = 1 - (a_1/a_2)^2 = e_{33}/(\pi\rho g a_2^2)$, $\sigma^2 = a_2\sigma^2/g$, $\overline{m} = m/(\pi\rho a_2^3) = \gamma d_2/a_2$, $\overline{\mu}_{33} = \mu_{33}/(\pi\rho a_2^3)$, and $\overline{\lambda}_{33} = \lambda_{33}/(\pi\rho\sigma a_2^3)$.

5 Optimal geometry

5.1 Computational method

Several computer codes are used to solve this optimization problem. The first one is the implementation of Chau and Yeung's [3] semi-analytical solution of the compound-cylinder hydrodynamic coefficients. This code yields the added mass, fluid damping, and wave exciting force (via Haskind's Relation) for a specific geometry (drafts and radii of cylinders) and frequency. Then the determination of the resonance frequency and RAO for a range of values of the outer draft and radius requires an iterative method as the hydrodynamic coefficients depend on the frequency.

Yeung's [2] semi-analytical resolution of the single-cylinder hydrodynamic coefficients is also implemented to determine the surge-and-pitch motion characteristics.

5.2 Optimal energy extraction

The maximal time-averaged mechanical power \overline{W}_{max} extracted by the device can be shown to be achieved at resonance[1], with:

$$\frac{\overline{W}_{max}}{A^2} = \frac{\pi}{8} \rho (a_2 g)^{3/2} \frac{|\overline{X}_3|^2}{\overline{\sigma}_{res} \overline{\lambda}_T}. \quad (13)$$

The capture width quantifies the width of the wave front from which energy is harnessed. With the use of Haskind's relation for \overline{X}_3 , one can show that³:

$$C_w = \frac{\overline{W}}{\frac{1}{2} \rho g A^2 V_g} = \frac{1}{(1 + f_{vis}) k_{res}}. \quad (14)$$

As a result, for a given resonance frequency (determined by the geometry of the device), the capture width will only depend on the viscous damping coefficient. It is noted that the expression derived for the average mechanical work is valid only when the floater heave motion is not restricted. If it were, the work done would be reduced [5].

5.3 Results

Heave motion of the outer cylinder: Figure 3 represents the Response Amplitude Operator as a function of the wave number, obtained for different geometries of the compound cylinder. A viscous coefficient f_{vis} of 10 has been applied to yield realistic values at resonance [1].

Surge and pitch motion: The resolution of the surge and pitch motion is implemented for the experimental compound-cylinder with equal drafts ($d_1 = d_2$). The mass characteristics (namely m_1 , m_2 , l_1 , l_2 , and $I_{\overline{O}}$) are determined from the CAD model. The results for a radius ratio $a_2/a_1 = 2.2$ are plotted in Fig. 4.

³ V_g is the group velocity of the wave.

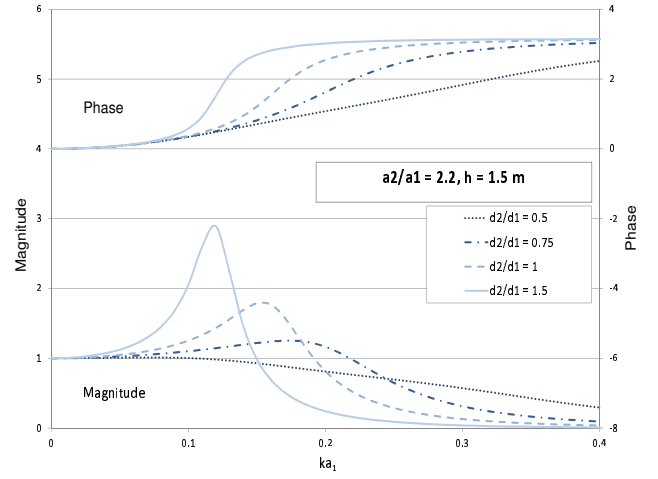


Figure 3: Magnitude and phase of the heave RAO as functions of the non-dimensional wave number ka_1 for different values of the geometrical parameter d_2/d_1 , and for $a_2/a_1 = 2.2$, $f_{vis} = 10$, with $h = 1.5$ m and $a_1 = 0.15$ m.

One observes, as expected, the existence of two coupled resonance frequencies. These resonance frequencies appear to be much lower than the resonance frequency of the heave motion for the outer cylinder. This validates the assumption that the compound cylinder does not experience any significant surge or pitch around the heave resonance frequency.

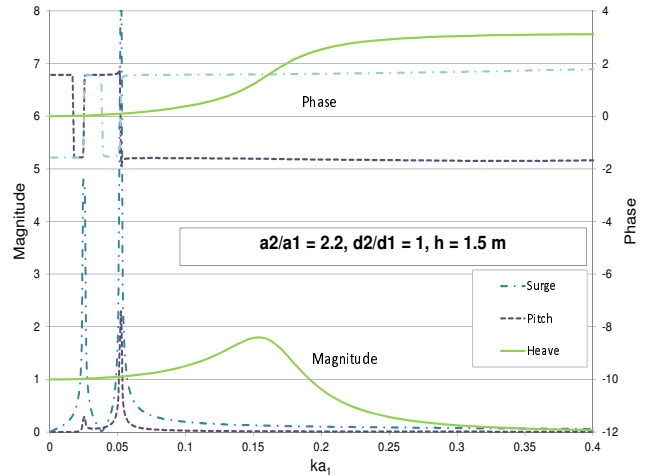


Figure 4: Magnitudes and phases, of the surge, heave and pitch RAOs as functions of the non-dimensional wave number ka_1 for $a_2/a_1 = 2.2$, $d_2/d_1 = 1$ and $f_{vis} = 10$, with $h = 1.5$ m and $a_1 = 0.15$ m.

Capture width: Figure 5 represents the capture width at resonance, normalized by the diameter of the outer cylinder, as a function of the non-dimensional wave number ka_1 , for different geometries. The values of the RAO are also reported to highlight the relation between RAO and capture width. One observes that a certain resonance frequency can be achieved by different $(a_2/a_1, d_2/d_1)$ combinations, but that the

highest normalized capture width will be obtained for a deep and narrow configuration (smaller radius ratio but larger draft ratio). Such a configuration leads to a smaller volume and wetted surface of the outer cylinder and thus a lower cost of material; however, it is limited by the neutral-buoyancy limit (buoyancy should balance the weight of the outer cylinder). The symbols on the graph (green dots) indicate when the neutral-buoyancy condition is met. On the other hand, a shallow-and-wide configuration would lead to smaller amplitudes of heave motion and would allow for larger wave amplitudes.

From Eqn.(13), one immediately notes that decreasing the viscous damping (described by f_{vis}) would linearly increase the capture width: for example, reducing f_{vis} from 10 to 5 would increase the capture width by a factor of $(1 + 10)/(1 + 5) = 1.85$. The viscous damping can be minimized by properly shaping the bottom of the outer cylinder [4].

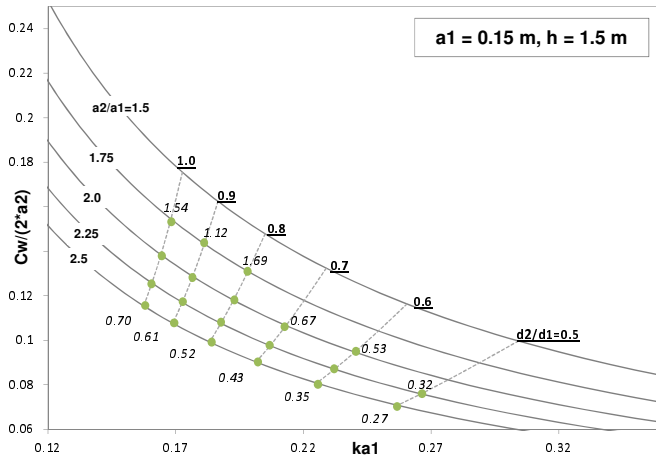


Figure 5: Capture width of the UCB design at resonance, normalized by $2a_2$, as a function of the non-dimensional wave-number ka_1 , for different values of the geometrical parameters a_2/a_1 and d_2/d_1 for a viscous damping coefficient $f_{vis} = 10$, with $h = 1.5 \text{ m}$ and $a_1 = 0.15 \text{ m}$. The values in italics indicate the RAO values and the dots the configurations for which the neutral-buoyancy condition of the outer cylinder is respected.

6 Conclusions

The wave-energy converter developed at UC Berkeley is modelled as a moored compound cylinder undergoing heave, surge and pitch motion. The inner cylinder is tethered in tension, while the outer cylinder is free to slide along the inner cylinder. The heaving motion of the outer cylinder is analysed and a systematic procedure is developed to analyse the effects of the geometric proportions on the capability of energy extraction.

With the use of multiple-body dynamics and linear-

wave theory, it is first shown that the surge and pitch degrees of freedom are decoupled from the heave motion. This latter is then studied independently to understand the influence of the geometrical parameters (draft and radius of the outer cylinder) on the extraction performance. The hydrodynamics properties of the outer cylinder in the presence of the inner one are obtained from a recently published work of the authors' laboratory.

It is observed that the maximization of the RAO leads to the maximization of the capture width. In this context, a smaller radius and deeper draft will lead to a larger capture width. In the experimental environment being planned, this statement holds up to a certain point, especially because the tank is of finite width and depth. Other physical considerations (e.g. generator characteristics) can also modify this statement.

With the coupled equations for the surge and pitch motion derived, the contact force and moment between the two cylinders can easily be computed. This would constitute the next logical step before the construction and testing of the device. Further improvements of the present work would also include a better modelling of the viscous effects, optimization of the bottom shape of the cylinders [4] and analysis of the dynamics in irregular waves [5].

References

- [1] R. W. Yeung, A. Peiffer, N. Tom, and T. Matlak. Design, analysis, and evaluation of the uc-berkeley wave-energy extractor. In *29th International Conference on Ocean, Offshore, and Arctic Engineering*, June 2010. Shanghai, China. (JOMAE link: <http://dx.doi.org/10.1115/1.4004518>)
- [2] R. W. Yeung. Added mass and damping of a vertical cylinder in finite-depth waters. *Applied Ocean Research*, 3(3):119–133, July 1981.
- [3] F. P. Chau and R. W. Yeung. Inertia and damping of heaving compound cylinders. In *25th International Workshop on Water Waves and Floating Bodies*, May 2010. Harbin, China.
- [4] R. W. Yeung and Y. Jiang. Effects of shaping on viscous damping and motion of heaving cylinders. In *30th International Conference on Ocean, Offshore, and Arctic Engineering*, June 2011. Rotterdam, The Netherlands.
- [5] M. J. Muliawan, Z. Gao, T. Moan, and A. Babarit. Analysis of a two-body floating wave energy converter with particular focus on the effects of power take-off and mooring systems on energy capture. In *30th International Conference on Ocean, Offshore and Arctic Engineering*, June 2011. Rotterdam, The Netherlands.